How much snow falls on the Antarctic ice sheet?

C. Palerme, J. E. Kay, C. Genthon, T. L'Ecuyer, N. B. Wood, C. Claud

The Cryosphere, 8, 1577–1587, 2014
www.the-cryosphere.net/8/1577/2014/
doi:10.5194/tc-8-1577-2014

The Cryosphere Open Access

How much snow falls on the Antarctic ice sheet?

C. Palerme[1,2], J. E. Kay[3], C. Genthon[1,2], T. L'Ecuyer[4], N. B. Wood[5], and C. Claud[6]

[1]CNRS, LGGE, UMR5183, 38041 Grenoble, France
[2]Univ. Grenoble Alpes, LGGE, UMR5183, 38041 Grenoble, France
[3]NCAR CGD – National Center for Atmospheric Research Climate and Global Dynamics, Boulder, Colorado, USA
[4]Department of Atmospheric and Oceanic Sciences, University of Wisconsin-Madison, Madison, Wisconsin, USA
[5]Cooperative Institute for Meteorological Satellite Studies, University of Wisconsin-Madison, Madison, Wisconsin, USA
[6]Laboratoire de Météorologie Dynamique/IPSL, CNRS, Ecole Polytechnique, Palaiseau, France

Correspondence to: C. Palerme (cyril.palerme@lgge.obs.ujf-grenoble.fr)

Received: 7 February 2014 – Published in The Cryosphere Discuss.: 24 February 2014
Revised: 3 July 2014 – Accepted: 16 July 2014 – Published: 22 August 2014

Abstract. Climate models predict Antarctic precipitation to increase during the 21st century, but their present day Antarctic precipitation differs. A model-independent climatology of the Antarctic precipitation characteristics, such as snowfall rates and frequency, is needed to assess the models, but it is not yet available. Satellite observations of precipitation by active sensors has been possible in the polar regions since the launch of CloudSat in 2006. Here, we use two CloudSat products to generate the first multi-year, model-independent climatology of Antarctic precipitation. The first product is used to determine the frequency and the phase of precipitation, while the second product is used to assess the snowfall rate. The mean snowfall rate from August 2006 to April 2011 is 171 mm year^{-1} over the Antarctic ice sheet, north of 82° S. While uncertainties on individual precipitation retrievals from CloudSat data are potentially large, the mean uncertainty should be much smaller, but cannot be easily estimated. There are no in situ measurements of Antarctic precipitation to directly assess the new climatology. However, distributions of both precipitation occurrences and rates generally agree with the European Centre for Medium-Range Weather Forecasts (ECMWF) ERA-Interim data set, the production of which is constrained by various in situ and satellite observations, but does not use any data from CloudSat. The new data set thus offers unprecedented capability to quantitatively assess Antarctic precipitation statistics and rates in climate models.

1 Introduction

Evaluating Antarctic snow accumulation, the sum of precipitation, sublimation/evaporation, meltwater run-off, and blowing snow (Eisen et al., 2008), is a major challenge with relevance to sea level rise. While no significant change in the total Antarctic snow accumulation has been found in ice cores and reanalysis products over the last 50 years (Monaghan et al., 2006a; Frezzotti et al., 2013), future changes are likely to occur, with global consequences: a projected 25 % increase in accumulation over the 21st century would result in a drop of approximately 160 mm per century in global sea level (Gregory and Huybrechts, 2006).

Climate models consistently predict Antarctic precipitation to increase in a warming climate (Church et al., 2013). However, their present day mean Antarctic precipitation differs widely, ranging from 150 to 550 mm year^{-1} in the CMIP3 archive (Genthon et al., 2009a). The Antarctic precipitation rates have also been evaluated from regional atmospheric models (Bromwich et al., 2004; Van de Berg et al., 2005; Monaghan et al., 2006b; Lenaerts et al., 2012). The mean solid precipitation rate over the grounded ice sheet reported by Van de Berg et al. (2005) is 164 mm year^{-1} using the model RACMO2/ANT. Moreover, Monaghan et al. (2006b) found a precipitation rate of 178 and 200 mm year^{-1} with Polar MM5 using the reanalysis NCEP-II and ERA40 respectively for the initial and boundary conditions. Reanalyses have also been used for assessing Antarctic precipitation (Monaghan et al., 2006a; Bromwich et al., 2011). Bromwich et al. (2011) have compared six reanalysis data sets and found

that the mean precipitation rate on the grounded ice sheet varies from 145 to 203 mm year^{-1}, depending on the reanalysis. There is, therefore, a need to document Antarctic precipitation from observations to benchmark climate models.

While accumulation rates have been assessed using in situ observations (Arthern et al., 2006; Eisen et al., 2008), characteristics of Antarctic precipitation (the dominant positive term of the accumulation), such as the frequency and rate, are still not well-known. Ground-based measurements are sparse and difficult to make in Antarctica. In coastal areas, katabatic winds are strong, which makes the distinction between blowing snow and precipitation difficult. On the Antarctic plateau, the annual accumulation is small (few centimeters per year, Bromwich et al., 2004), and the instrumentation must be able to detect very light precipitation. In addition, low temperatures and hoarfrost negatively impact instruments that are not designed for harsh environments.

Precipitation characteristics depend greatly on the region in Antarctica. In coastal areas, precipitation is influenced by synoptic scale features, such as cyclones and fronts (Bromwich, 1988). In the interior (> 2500 m), a potentially significant part of the precipitation falls in the form of "diamond dust" (ice crystals) under clear-sky conditions (Bromwich, 1988; Fujita and Abe, 2006).

In the past, passive microwave remote sensing has been used to detect new snow accumulation, using changes in surface emissivity (Bindschadler et al., 2005). However, the method was not quantitative, and was found to be affected by other processes, such as temperature and surface roughness.

Observations from the cloud-profiling radar (CPR) on CloudSat provide the first opportunity to estimate precipitation in polar regions from a spaceborne radar (Stephens et al., 2008; Liu, 2008). With data available from August 2006 to April 2011, CloudSat directly observes snow precipitating through the atmosphere, rather than after it has been accumulated on the surface. Several algorithms have been tested for precipitation over polar regions using CloudSat (Kulie and Bennartz, 2009; Hiley et al., 2010). Moreover, Boening et al. (2012) have already shown that there is good agreement between CloudSat, GRACE, and ERA-Interim for Antarctic precipitation variability over Dronning Maud Land (30° W–60° E, and 65–80° S). However, no precipitation climatology has been done over Antarctica on the continent scale. In this study, we used two CloudSat products to make the first multi-year climatology of Antarctic precipitation north of 82° S from spaceborne observations.

2 Data and methods

The CPR, onboard CloudSat, is a nadir-looking radar at 94 GHz that measures the power backscattered by cloud particles and hydrometeors according to the distance from the sensor. It provides radar reflectivity profiles divided into 150 bins at a vertical resolution of 240 m, with a 1.7 km $\times$ 1.3 km footprint, and up to 82° of latitude. Its minimum detectable radar reflectivity is around -28 dBZ.

In this study, two CloudSat products are used to determine the characteristics of Antarctic precipitation. The first product, 2C-PRECIP-COLUMN (Haynes et al., 2009), is used to assess the phase and occurrence frequency of Antarctic precipitation. 2C-PRECIP-COLUMN provides a precipitation flag based on the near-surface reflectivity (dBZ) at the fourth bin over the ocean (between 600 and 840 m above the surface), and at the sixth bin over land (about 1300 m) to remove surface contamination (ground clutter). The radar bin containing the surface is determined with a digital elevation model. The phase is obtained using the temperature at 2 m predicted by the European Centre for Medium-Range Weather Forecasts (ECMWF) operational weather analysis, and a model of melting layer with a constant lapse rate of 6 °C km^{-1}. According to the phase, different thresholds are applied to the near surface reflectivity to determine a likelihood of precipitation (possible or certain). Thus, the precipitation flags inform about the likelihood and the phase of precipitation.

The second product, 2C-SNOW-PROFILE (Wood, 2011; Wood et al., 2013) is used to assess the snowfall rates. 2C-SNOW-PROFILE retrieves estimates of liquid-equivalent snowfall rate for profiles where 2C-PRECIP-COLUMN indicates "snow possible" or "snow certain", or where 2C-PRECIP-COLUMN indicates "mixed possible" or "mixed certain", and the estimated melted mass fraction at the surface is less than or equal to 0.1. Using a priori estimates of snow particle size distribution, microphysical and scattering properties, an optimal estimation retrieval (Rodgers, 2000) is performed for the contiguous layer of snow-containing radar bins nearest the surface, with exclusions for likely ground clutter contamination. With this approach, the so-called Z–S relationship between radar reflectivity and snowfall rate is not fixed, but can vary subject to the constraints of the reflectivity profile and the a priori expectations.

The retrieval also provides estimates of uncertainties for the retrieved snowfall rates. The uncertainties depend on the uncertainties in the observed reflectivities, as well as those in the simulated reflectivities provided by the retrieval's radar forward model. These uncertainties arise due to measurement error and due to the approximate nature of the forward model and its a priori assumptions. To the extent to which they can be characterized, systematic errors are removed. Within the context of the retrieval algorithm, the remaining uncertainties are considered to be unbiased and random. However, these likely consist of some combination of systematic and random uncertainties since, for example, the algorithm's a priori assumptions are not tuned to the particular characteristics of Antarctic snowfall. Thus, while multi-year averaging of retrieved snowfall rates reduces the truly random component of the uncertainties, some indeterminate bias is likely also present, and its evaluation is an ongoing area of research.

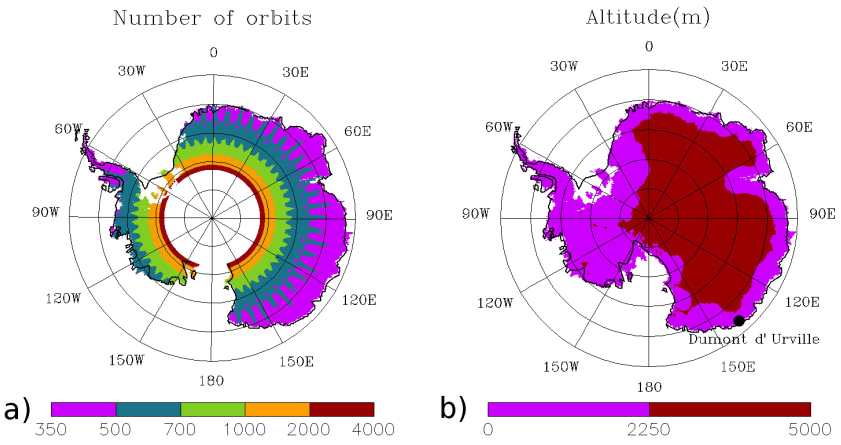

Figure 1. (a) Total number of orbits per grid cell from August 2006 to April 2011. **(b)** The 2250 m elevation contour derived from the digital elevation model of Bamber et al., 2009. The part of the ice sheet with surface elevation over 2250 m (red), and below 2250 m (purple). The black dot indicates the location of Dumont d'Urville station.

In this study, both CloudSat data sets are processed over a grid of 1° of latitude by 2° of longitude between 63 and 82° S. The number of orbits per grid cell for the period August 2006–April 2011 is shown in Fig. 1. Over the Antarctic continent, the number of orbits per grid cell is at least 350 for the entire period, which represents one orbit every 5 days. It does not seem to be an issue to produce a climatology of precipitation (Fig. 5, discussed below). The ratio of the surface directly observed by CloudSat over the surface of the ice sheet is shown in Fig. S1 in the Supplement. Even for latitudes less than 82° S, the surface directly covered by CloudSat is only a fraction of the total surface of the ice sheet. However, the spatial scale of precipitation events and the overpass frequency ensure adequate statistical sampling over the duration of the study (Supplement Fig. S1).

CloudSat products provide the data along their orbit. In order to map the 2C-PRECIP-COLUMN data over a grid of 1° by 2°, one sample per grid-cell overflown is retained for each orbit. Thus, we redefined new samples from the original 2C-PRECIP-COLUMN flags. First, for the precipitation frequency, flags are sorted into three classes: "no precipitation", "precipitation possible", and "precipitation certain". Then, if all the flags in the same grid cell indicate no precipitation, no precipitation is retained. If at least one flag indicates precipitation certain in the grid cell, precipitation certain is retained. And if there is no flag indicating precipitation certain, and at least one flag indicating precipitation possible, precipitation possible is retained. It is relevant to note that this method tends to inflate the precipitation occurrence.

To map the precipitation phase, flags are sorted into four classes: "no precipitation", "liquid", "mixed", and "solid precipitation". If the flags in the grid cell indicate no precipitation and precipitation, but only one precipitation phase, this phase is retained. If the flags in the same grid cell indicate rain and mixed precipitation, mixed precipitation and snow, or rain and snow, mixed precipitation is retained. For the precipitation phase, this method tends to inflate the mixed precipitation class. For the snowfall rate and its uncertainty from the 2C-SNOW-PROFILE product, the mean value in the grid cell has been retained for each orbit.

CloudSat observations have been compared to ERA-Interim reanalysis in this study. ERA-Interim is the latest global atmospheric reanalysis produced by the ECMWF (Simmons et al., 2006; Dee et al., 2011). ERA-Interim provides data from 1979 to present at a 6-hourly resolution. Its coverage is global at a spatial resolution of about $0.75° \times 0.75°$. The 6 and 12 h forecasts of precipitation are used here. Data from surface observations and radiosondes, commercial aircraft observations, and satellites measurements are assimilated in the numerical model to improve and constrain the forecasts (Dee et al., 2011). Direct precipitation observations are not assimilated into the model, but precipitation is influenced by the four-dimensional variational assimilation of other variables, such as temperature and humidity (http://www.ecmwf.int).

ERA-Interim has been chosen in this study because it likely offers the most realistic depiction of Antarctic precipitation variability among reanalyses (Bromwich et al., 2011). However, it has been shown that ERA-Interim could have a dry bias over the East Antarctic plateau (Bromwich et al., 2011; Favier et al., 2013).

3 Results

3.1 Precipitation characteristics from CloudSat

Figure 2 shows two maps of the precipitation frequency assessed from the 2C-PRECIP-COLUMN flags, and a map of the ratio of the number of samples indicating precipitation possible over the number of samples indicating precipitation possible and certain. Map **(a)** represents the proportion

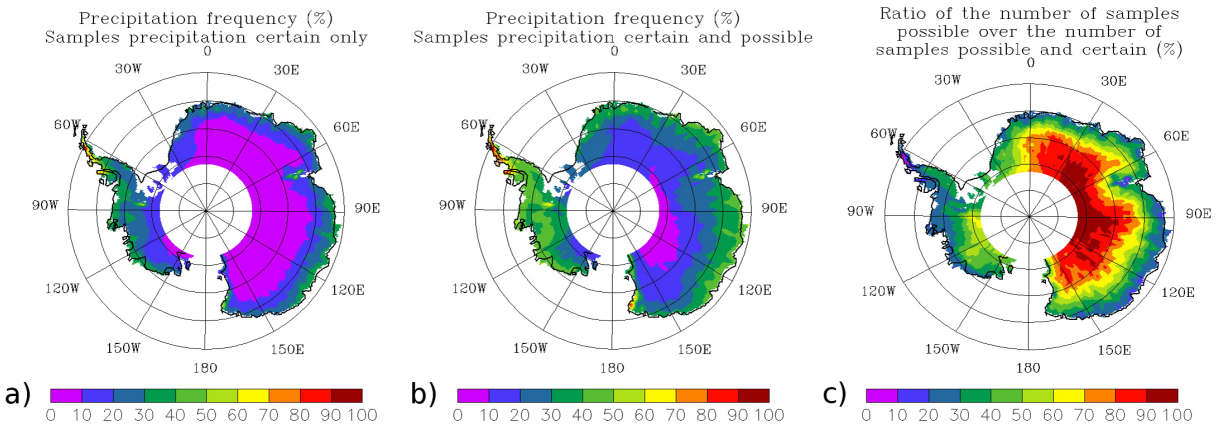

Figure 2. (a) Precipitation frequency (%) with the samples indicating precipitation certain for the period August 2006–April 2011. **(b)** Precipitation frequency (%) with the samples indicating precipitation certain and possible for the period August 2006–April 2011. **(c)** Ratio of the number of samples indicating precipitation possible over the number of samples indicating precipitation certain and possible.

of samples indicating precipitation certain, and map **(b)**, the proportion of samples indicating precipitation certain and possible.

The mean precipitation frequency (% of time) observed by CloudSat over the Antarctic continent (latitude $< 82°$ S) is 14 % when the samples precipitation possible are not taken into account, and 26 % with the samples precipitation possible included. The spatial pattern of the precipitation frequency shows two distinct regions. The first area includes the West Antarctic ice sheet and the peripheral part of the East Antarctic ice sheet, which corresponds approximately to the part of the continent with surface elevation below 2250 m. In this region, relatively high precipitation frequency is observed by CloudSat (between 22 and 34 %, depending on whether the samples precipitation possible are taken into account). The second region is the Antarctic plateau in East Antarctica (with surface elevation > 2250 m), where the precipitation frequency observed by CloudSat is much lower (between 5 and 19 %). Figure 1 shows the parts of the ice sheet with surface elevation over and below 2250 m, derived from combined satellite radar and laser data (Bamber et al., 2009). Each part represents 50 % of the surface of the Antarctic ice sheet (including the part of the continent between 82 and 90° S).

In Fig. 2, map **(c)** shows the number of samples indicating precipitation possible over the number of samples indicating precipitation possible and certain. While over the periphery of the ice sheet, most of the precipitation events detected are sorted as certain, most of the samples indicating precipitation are sorted as possible in the interior. Near-surface reflectivity is sensitive to the size of hydrometeors, and on the plateau, particles are probably too small to increase the near-surface reflectivity above the threshold precipitation certain. The reflectivity thresholds applied in this algorithm could be too high for this kind of precipitation.

Precipitation phase has also been studied from the 2C-PRECIP-COLUMN flags. Only samples indicating precipitation certain were taken into account. Over the Antarctic ice sheet (latitude $< 82°$ S), solid precipitation represents 99.60 %, mixed precipitation 0.32 %, and rain 0.08 % of the precipitation occurrence (similar results have been found with the samples indicating precipitation possible included). In peripheral areas (surface elevation < 2250 m), mixed precipitation represents 0.63 % and rain 0.15 % of the precipitation occurrence. Relatively more liquid and mixed precipitation occurs over the Peninsula compared to the rest of the ice sheet (mixed precipitation represents 4.10 %, and rain 1.32 % of the precipitation occurrence over this region). Furthermore, on the Antarctic plateau (surface elevation > 2250 m), all the precipitation is solid.

Because snowfall rate in the 2C-SNOW-PROFILE product is only estimated when the melted fraction is assessed to be less than or equal to 0.1, this product is well-suited to examining precipitation over Antarctica. Figure 3 shows the mean annual snowfall rate, the single retrieval snowfall rate uncertainty, and the ratio of the single retrieval uncertainty over the snowfall rate from the 2C-SNOW-PROFILE data. The mean snowfall rate observed by CloudSat on the Antarctic continent (latitude $< 82°$ S) is 171 mm water equivalent (w.e.) per year. However, the spatial pattern of the snowfall rate shows considerable differences between West Antarctica and East Antarctica. In West Antarctica, the mean annual snowfall rate is 303 mm w.e. per year, compared to 118 mm w.e. per year in East Antarctica. Furthermore, the mean snowfall rate over the peripheral part of the ice sheet (with surface elevation < 2250 m) is 303 mm w.e. per year, compared to 36 mm w.e. per year for the interior of the ice sheet (with surface elevation > 2250 m).

The map of the snowfall rate uncertainty in Fig. 3 represents the mean value of the single retrieval uncertainty for all the snowfall rate retrievals from August 2006 to April 2011.

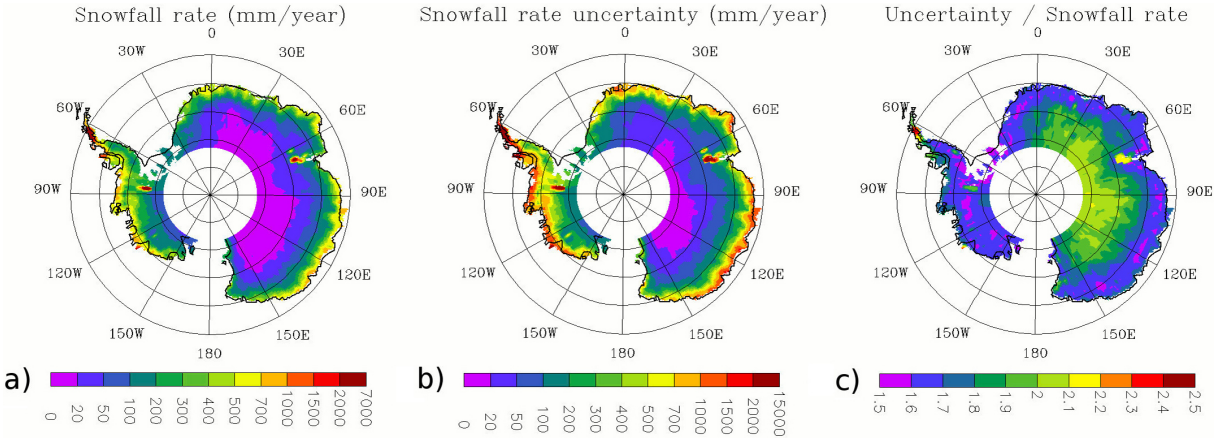

Figure 3. (a) Mean annual snowfall rate (mm water equivalent/year) from the 2C-SNOW-PROFILE product for the period August 2006–April 2011. **(b)** Mean single retrieval uncertainty from the 2C-SNOW-PROFILE product for the period August 2006–April 2011. **(c)** The ratio of the single retrieval uncertainty over the snowfall rate.

These are the expected uncertainties for individual snowfall rate retrievals and, as noted earlier, likely consist of both random and systematic components. Considering the maps in Fig. 3, 2C-SNOW-PROFILE product provides a snowfall rate uncertainty between 1.5 and 2.5 times the snowfall rate for 4.7 years of certain data accumulated on the $1° \times 2°$ grid boxes. This relative uncertainty is particularly high on the Antarctic plateau and the Peninsula, and it is lower on the peripheral part of the ice sheet and in West Antarctica. When calculating mean values with a large number of observations, the standard error of the mean decreases as the number of samples increases. Therefore, in this study, the uncertainty of a 4.7-year mean snowfall rate should be fairly small. However, the real snowfall rate uncertainty on the entire CloudSat period is difficult to assess because the relative contribution of systematic and random errors remains unknown.

3.2 Comparison of the CloudSat products to ERA-Interim reanalysis

Table 1 shows a comparison between ERA-Interim reanalysis and the precipitation samples from CloudSat at the French station Dumont d'Urville (Fig. 1). The nearest grid cell of the ERA-Interim reanalysis has been taken into account for comparing the data sets. The ability of ERA-Interim to represent precipitation in Antarctica is not yet well-known, but it is expected that observations assimilated in the model help to constrain the forecasts. It is important to note that CloudSat observations are not used to produce ERA-Interim reanalysis (Dee et al., 2011). Surface observations and radiosoundings are performed at Dumont d'Urville and assimilated in ERA-Interim. Humidity profiles, obtained by radiosounding, influence the forecasts used to predict precipitation in ERA-Interim. Therefore, precipitation predicted by ERA-Interim should be relatively more reliable at Dumont d'Urville than at other sites, where no observation is available.

Table 1. Comparison between the precipitation samples from CloudSat and ERA-Interim reanalysis at Dumont d'Urville for the period August 2006–April 2011. In ERA-Interim reanalysis, precipitation events were defined for a precipitation rate over 0.07 mm per 6 h. The success rate is the proportion of samples indicating a situation (precipitation/no precipitation) that match the same situation in ERA-Interim. For the precipitation possible, the success rate is the proportion of samples indicating precipitation possible that match precipitation events in ERA-Interim.

Detection	Number of samples	Success rate
Period without precipitation	265	92 %
Precipitation certain	85	91 %
Precipitation possible	38	55 %

Comparisons of the ERA-Interim reanalysis data at Dumont D'Urville station against the precipitation samples from CloudSat were used to establish a precipitation rate threshold for comparing the data sets. This threshold is necessary because the ERA-Interim precipitation rates were strictly positive 60 % of the time between 2006 and 2011 at Dumont D'Urville station (for comparison, the precipitation frequency from CloudSat at Dumont d'Urville is between 22 and 32 %). A threshold of 0.07 mm per 6 h for the ERA-Interim precipitation rates was found empirically to give good agreement with the CloudSat precipitation samples; 0.07 mm per 6 h corresponds to the threshold for which the highest Heidke skill score (Barnston, 1992) has been obtained.

From 2006 to 2011, 67 % of the time, the ERA-Interim precipitation rates at Dumont D'Urville were below this rate. During this period, for the 265 samples that indicate no precipitation, 92 % match with no precipitation in ERA-Interim. Furthermore, for the 38 samples indicating precipitation

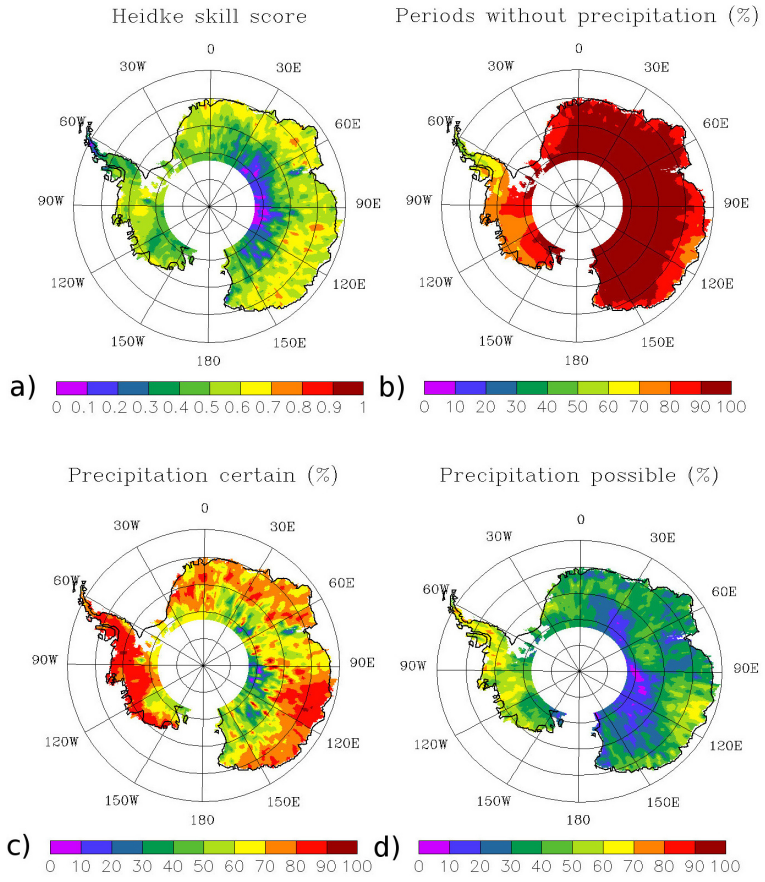

Figure 4. Comparison between the precipitation samples from CloudSat and ERA-Interim reanalysis for the period August 2006–April 2011. In ERA-Interim reanalysis, precipitation events were defined for a precipitation rate over 0.07 mm per 6 h. **(a)** Heidke skill score assessed using samples indicating precipitation certain and period without precipitation. **(b)** Proportion of samples indicating periods without precipitation that match periods without precipitation in ERA-Interim. **(c)** Proportion of samples indicating precipitation certain that match precipitation events in ERA-Interim. **(d)** Proportion of samples indicating precipitation possible that match precipitation events in ERA-Interim.

possible, 55 % match with a precipitation event in ERA-Interim. And for the 85 samples indicating precipitation certain, the success rate was 91 %.

A similar comparison at the continent scale is shown in Fig. 4. To compare the data sets, ERA-Interim reanalyses have been interpolated on the same $1° \times 2°$ grid as CloudSat. The threshold used in ERA-Interim was the same as for Dumont d'Urville (0.07 mm/6 h). The value of the appropriate threshold seems to depend on the location in Antarctica, and it is probably lower where the precipitation rate is small.

The method used for determining the threshold at Dumont d'Urville (highest Heidke skill score obtained for this threshold) has been tested in the interior of the ice sheet. This method tends to maximize the success rate of the different classes according to the number of samples in each class. Because there are less samples indicating precipitation certain in the interior of the ice sheet compared to the total number of samples (Fig. 2c), it tends to maximize the success rate for the class "periods without precipitation". Thus, the threshold in the interior of the ice sheet tends to be higher than 0.07 mm per 6 h, while the precipitation rate is smaller in this region. That is why we chose to keep the same threshold for the whole continent as that determined at Dumont d'Urville.

Overall, the success rate for the samples precipitation certain and precipitation possible is better near the coast than in the interior of the ice sheet. It could be due to the threshold applied to ERA-Interim precipitation, which could be too high for the Antarctic interior. Moreover, shallow precipitation missed by CloudSat, and the weak reflectivity of small hydrometeors in the interior, could contribute to this difference.

Figure 4 also shows a map of the Heidke skill score. The Heidke skill score measures the accuracy of forecasts relative to random forecasts (Barnston, 1992). It can vary between -1 and 1. A Heidke skill score equal to 0 means that forecasts are as good as random, and it is equal to 1 for perfect forecasts. If the Heidke skill score is positive,

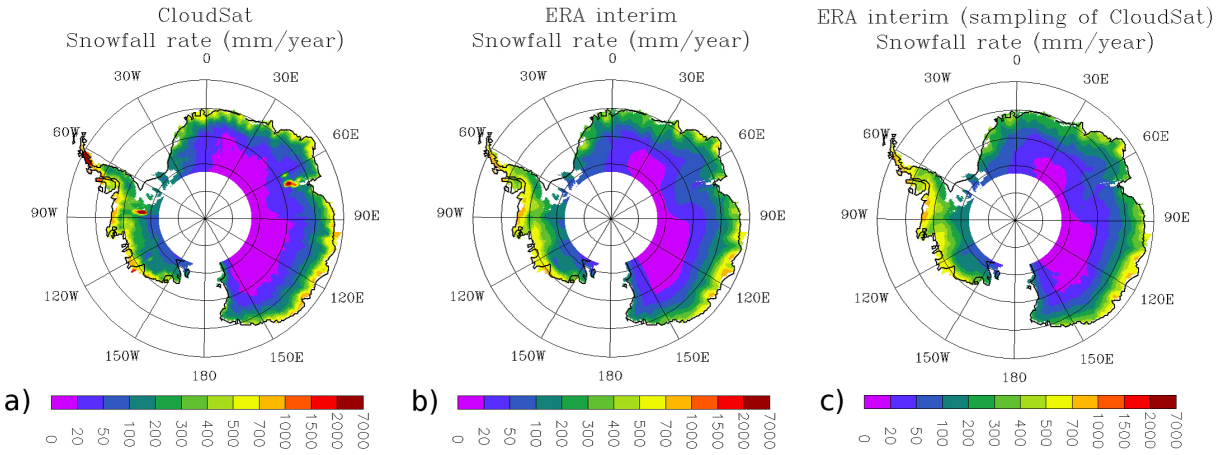

Figure 5. (a) Mean annual snowfall rate (mm water equivalent/year) from CloudSat from August 2006 to April 2011. **(b)** Mean annual snowfall rate (mm water equivalent/year) from ERA-Interim reanalysis from August 2006 to April 2011. **(c)** Mean annual snowfall rate (mm water equivalent/year) from ERA-Interim with the same temporal sampling as CloudSat.

Table 2. Comparison between the snowfall rate (mm year^{-1}) from CloudSat and ERA-Interim reanalysis for the period August 2006–April 2011, and the accumulation rate (mm year^{-1}) from Arthern et al. (2006) for the period 1950–2000. All the rates given in this table are averaged over the surface observed by CloudSat (latitude $< 82°$ S).

	Continent	Altitude > 2250 m	Altitude < 2250 m
Snowfall rate from CloudSat	171	36	303
Snowfall rate from ERA-Interim	163	49	273
Snowfall rate from ERA-Interim (sampling of CloudSat)	163	53	271
Accumulation rate from Arthern et al.	163	81	243

the forecasts are better than random forecasts. Here, samples indicating precipitation certain and period without precipitation are used. Figure 4 shows better agreement between CloudSat and ERA-Interim (higher Heidke skill score) over peripheral areas than over the interior.

Even if precipitation is not assimilated in ERA-Interim, observations assimilated, such as humidity profiles, are more numerous in peripheral areas than in the Antarctic interior. Observations of wind, pressure, and temperature further help constrain the strength and timing of the perturbations and thus that of the precipitation events. Perturbations are fainter when they reach the interior and, as there are less observations available, they are less efficient at controlling the occurrence and timing of precipitation through assimilation. Therefore, ERA-Interim should be more reliable in peripheral areas than on the Antarctic plateau. This could help explain why there is better agreement between CloudSat and ERA-Interim in peripheral areas than in the interior of the ice sheet. However, agreement between CloudSat and ERA-Interim is good over West Antarctica, where there are less observations assimilated than over peripheral areas of East Antarctica. Overall, there is better agreement where the snowfall rate is high.

A comparison between the snowfall rate observed by CloudSat and simulated by ERA-Interim is shown in Fig. 5 and in Table 2. For this comparison, a map with the same temporal sampling as CloudSat has been created. Every time a grid cell has been overflown by CloudSat, the corresponding time step in ERA-Interim has been retained. This data set has been created in order to test if the temporal sampling of CloudSat may result in a bias for the period August 2006–April 2011.

The snowfall rates from ERA-Interim with the same temporal sampling as CloudSat and from the full ERA-Interim data set are similar (163 mm w.e. per year for both data sets over the Antarctic continent north of 82° S). The snowfall rate from ERA-Interim with the same temporal sampling as CloudSat is slightly stronger over the interior of the ice sheet (53 compared to 49 mm w.e. per year), and slightly lower over the periphery (271 compared to 273 mm w.e. per year). These are considered marginal differences, and temporal sampling of CloudSat does not seem to be an issue.

Over the Antarctic continent (latitude $< 82°$ S), the mean snowfall rate is 171 mm w.e. per year for CloudSat and 163 mm w.e. per year for ERA-Interim. The snowfall rate observed by CloudSat and predicted by ERA-Interim are relatively similar over the ice sheet, except over parts of the

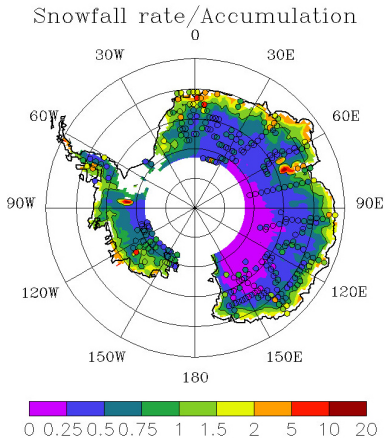

Figure 6. Map: ratio of the snowfall rate observed by CloudSat for the period August 2006–April 2011 over the accumulation rate determined by Arthern et al. (2006) for the period 1950–2000 (the isoline 1 is shown on the map). Dots: ratio of the snowfall rate observed by CloudSat for the period August 2006–April 2011 over the accumulation rate from Favier et al. (2013).

Peninsula, the Vinson massif (78° S, 85° W), and the Prince Charles Mountains (around 72° S, 65° E), where the snowfall rate from CloudSat is significantly stronger. Orographic precipitation could be seen by CloudSat, but not predicted by ERA-Interim due to the difference in spatial resolution between both data sets. However, ground clutter should be stronger over mountainous areas than over flat terrain, and may induce a spuriously high snowfall rate.

3.3 Comparison of the snowfall rate from CloudSat to surface mass balance observations

Table 2 and Fig. 6 show a comparison between the snowfall rate obtained by CloudSat for the period August 2006–April 2011, and the accumulation rate assessed by Arthern et al. (2006) for the period 1950–2000. Arthern et al. (2006) used in situ glaciological measurements to assess the accumulation, and passive radiometer data (AMSR-E) which are sensitive to snowpack characteristics for interpolating their results.

Assuming that accumulation has not significantly changed during the last 50 years (Monaghan et al., 2006a; Frezzotti et al., 2013), the accumulation from Arthern et al. (2006) represents 95 % of the snowfall over the Antarctic ice sheet north of 82° S. The snowfall rate observed by CloudSat is higher than the accumulation over the periphery of the ice sheet, which is expected due to the negative contribution to accumulation of sublimation, melt/run-off, and blowing snow.

However, the snowfall rate observed by CloudSat is lower than the accumulation in the interior. Snowfall rate assessed by CloudSat over the interior of the ice sheet may be underestimated due to shallow precipitation missed by CloudSat and the weak reflectivity of small hydrometeors. Additionally, modeling studies have suggested that deposition (inverse sublimation) could be stronger than evaporation at some locations in the interior of the ice sheet (Genthon and Krinner, 2001). Thus, hoarfrost formation could contribute significantly to the accumulation, and precipitation could be lower than accumulation in these regions.

Ground-based measurements used to produce the accumulation map from Arthern et al. (2006) were not filtered according to their accuracy, and some measurements have been found to be unreliable (Magand et al., 2007). Genthon et al. (2009b) have shown that the unreliability of some in situ observations used by Arthern et al. (2006) would lead to an overestimated accumulation in the interior of the ice sheet. Thus, the accumulation from Arthern et al. (2006) could be overestimated in this region. Moreover, Magand et al. (2008) have shown that the interpolation based on microwave surface emission used by Arthern et al. (2006) can be inaccurate in coastal areas affected by melt during the summer.

Favier et al. (2013) assembled a surface mass balance database in which ground-based measurements have been sorted into three classes according to their accuracy. Observations sorted in the most reliable class for the 20th century by Favier et al. (2013) have been used in this study. The ratio of the snowfall rate observed by CloudSat over the accumulation from Favier et al. (2013) is reported on the map of Fig. 6. When several values of accumulation are given in the database of Favier et al. (2013) for the same grid cell of $1° \times 2°$, the mean value for the grid cell is shown in Fig. 6. Overall, the comparison between the snowfall rate from CloudSat and the accumulation from Favier et al. (2013) confirms the results from the comparison with the accumulation map of Arthern et al. (2006). However, in some grid cells, accumulation is not spatially homogeneous, and a few in situ measurements can sometimes be non-representative of the mean accumulation in the grid cell. For instance, there is only one value of accumulation for the three red dots of Fig. 6 showing the largest ratio between the snowfall rate from CloudSat and the accumulation from Favier et al. (2013).

4 Discussion and conclusion

A climatology of the Antarctic precipitation, the single most important positive term of the ice sheet mass balance, has yet to be established from observations. Filling this gap, Antarctic precipitation features such as the frequency, the phase, and the snowfall rate have been determined here using CloudSat products. CloudSat is the first spaceborne radar to be able to observe precipitation in Antarctica (Boening et al., 2012), and its potential is confirmed here. The mean snowfall rate from August 2006 to April 2011 is 171 mm year^{-1} over the Antarctic ice sheet north of 82° S. Expectedly, the observed surface accumulation of snow is, on average, less than snowfall. However, it appears to exceed snowfall in areas of lesser

precipitation, where uncertainties on both precipitation and accumulation reports are largest. A significant contribution of hoarfrost to the surface mass balance of these areas may not be excluded.

However, due to assumptions about particle size distribution, particle masses, shapes, and fall speeds, snowfall rates assessed in the 2C-SNOW-PROFILE product have large uncertainties. In the 2C-PRECIP-COLUMN data set, a large number of samples are sorted as "precipitation possible". This leads to a considerable range of precipitation frequency, even if the frequency estimated is probably more reliable than the snowfall rate. Moreover, on the Antarctic plateau, the 2C-PRECIP-COLUMN algorithm may have difficulties in distinguishing precipitating from non-precipitating hydrometeors due to their small particle size.

CloudSat is likely more accurate in peripheral areas than in the interior. Shallow precipitation (< 1300 m), missed by CloudSat, could be an important contribution to precipitation on the Antarctic plateau. Therefore, the precipitation frequency and the snowfall rate could be underestimated over this region. Conversely, because near surface reflectivity is measured about 1300 m over the surface, blowing snow is not confounded with precipitation in peripheral areas, which is usually the main problem for precipitation measurements over this region.

Due to the difficulties for CloudSat in detecting precipitation in the interior of the ice sheet, CloudSat precipitation products are more useful in the periphery of the ice sheet than in the interior. However, precipitation in the periphery of the ice sheet is quite important. Three quarters of the total Antarctic precipitation falls in this region, and it is where the models predict the largest precipitation increase over the 21st century (Genthon et al., 2009a).

The lack of ground-based measurements prevents direct validation of CloudSat data. Nevertheless, agreement between CloudSat data and ERA-Interim reanalysis is encouraging for reliability of both data sets. This is consistent with the study of Boening et al. (2012), who have already found good agreement between CloudSat and ERA-Interim for the snowfall rate in Antarctica in the region 30° W–60° E, 65–80° S. Even if the spatiotemporal sampling of CloudSat is relatively low (between 350 and 500 orbits per grid cell over the Antarctic periphery for the period August 2006–April 2011), the snowfall rate obtained with CloudSat is similar to the snowfall rate predicted by ERA-Interim during the same period (Fig. 5). Therefore, the spatiotemporal sampling of CloudSat seems to be sufficient to reproduce characteristics of Antarctic precipitation for the period August 2006–April 2011. In extrapolating CloudSat snowfall observations to the region south of 82° S using ERA-Interim data, the mean snowfall rate over the full Antarctic ice sheet amounts to 148 mm year^{-1}.

CloudSat does not provide any data during the night since April 2011. The EarthCARE satellite scheduled for launch in 2015 into a polar orbit will carry a CPR (Kumagai et al., 2003). In addition to the reflectivity profiles, EarthCARE will measure the vertical Doppler velocity, which will allow access to new information about the cloud particles. Moreover, it will have a better sensitivity than CloudSat (-35 dBZ, compared to -28 dBZ for CloudSat), and a better sampling interval (100 m, compared to 250 m for CloudSat) (Nakatsuka et al., 2008). In situ observations are highly desirable to evaluate and improve remote sensing techniques for Antarctic precipitation studies, and could be very useful during the EarthCARE mission. Future spaceborne radar missions should allow us to determine whether Antarctic precipitation is increasing due to global warming, as predicted by models.

The Supplement related to this article is available online at doi:10.5194/tc-8-1577-2014-supplement.

Acknowledgements. This study was supported by the LEFE/CLAPA programme (Institut National des Sciences de l'Univers). This work was partially supported by funding from the ICE2SEA programme of the European Union 7 framework programme, grant number 226375. Ice2Sea contribution number 176. Funding for this project was provided by a grant from la Région Rhône-Alpes. We are grateful to the Observatoire des Sciences de l'Univers de Grenoble (OSUG), who provided funding for visits around France and the USA. Parts of this research by N. B. Wood and T. L'Ecuyer were performed at the University of Wisconsin-Madison for the Jet Propulsion Laboratory, California Institute of Technology, sponsored by the National Aeronautics and Space Administration. CloudSat data were obtained from the CloudSat Data Processing Center (http://www.cloudsat.cira.colostate.edu). Finally, we thank the two anonymous reviewers for their comments which significantly improved the manuscript.

Edited by: M. van den Broeke

References

Arthern, R. J., Winebrenner, D. P., and Vaughan, D. G.: Antarctic snow accumulation mapped using polarization of 4.3-cm wavelength microwave emission, J. Geophys. Res.-Atmos., 111, D06107, doi:10.1029/2004JD005667, 2006.

Bamber, J. L., Gomez-Dans, J. L., and Griggs, J. A.: A new 1 km digital elevation model of the Antarctic derived from combined satellite radar and laser data –Part 1: Data and methods, The Cryosphere, 3, 101–111, doi:10.5194/tc-3-101-2009, 2009.

Barnston, A. G.: Correspondence among the Correlation, RMSE, and Heidke Forecast Verification Measures; Refinement of the Heidke Score, Weather Forecast., 7, 699–709, 1992.

Bindschadler, R., Choi, H., Shuman, C., and Markus, T.: Detecting and measuring new snow accumulation on ice sheets by satellite remote sensing, Remote Sens. Environ., 98, 388–402, 2005.

Boening, C., Lebsock, M., Landerer, F., and Stephens, G.: Snowfall-driven mass change on the East Antarctic ice sheet, Geophys. Res. Lett., 39, L21501, doi:10.1029/2012GL053316, 2012.

Bromwich, D. H.: Snowfall in high southern latitudes, Rev. Geophys., 26, 149–168, 1988.

Bromwich, D. H., Guo, Z., Bai, L., and Chen, Q.-S.: Modeled Antarctic Precipitation. Part I: Spatial and Temporal Variability, J. Climate, 17, 427–447, 2004.

Bromwich, D. H., Nicolas, J. P., and Monaghan, A. J.: An Assessment of Precipitation Changes over Antarctica and the Southern Ocean since 1989 in Contemporary Global Reanalyses*, J. Climate, 24, 4189–4209, doi:10.1175/2011JCLI4074.1, 2011.

Church, J. A., Clark, P. U., Cazenave, A., Gregory, J. M., Jevrejeva, S., Levermann, A., Merrifield, M. A., Milne, G. A., Nerem, R. S., Nunn, P. D., Payne, A. J., Pfeffer, W. T., Stammer, D., and Unnikrishnan, A. S.: Sea Level Change, in: Climate Change 2013: The Physical Science Basis. Contribution of Working Group I to the Fifth Assessment Report of the Intergovernmental Panel on Climate Change, edited by: Stocker, T. F., Qin, D., Plattner, G. K., Tignor, M., Allen, S. K., Boschung, J., Nauels, A., Xia, Y., Bex, V., and Midgley, P. M., Cambridge University Press, Cambridge, United Kingdom and New York, NY, USA, 2013.

Dee, D. P., Uppala, S. M., Simmons, A. J., Berrisford, P., Poli, P., Kobayashi, S., Andrae, U., Balmaseda, M. A., Balsamo, G., Bauer, P., Bechtold, P., Beljaars, A. C. M., van de Berg, L., Bidlot, J., Bormann, N., Delsol, C., Dragani, R., Fuentes, M., Geer, A. J., Haimberger, L., Healy, S. B., Hersbach, H., Hólm, E. V., Isaksen, L., Kållberg, P., Köhler, M., Matricardi, M., McNally, A. P., Monge-Sanz, B. M., Morcrette, J.-J., Park, B.-K., Peubey, C., de Rosnay, P., Tavolato, C., Thépaut, J.-N., and Vitart, F.: The ERA-Interim reanalysis: configuration and performance of the data assimilation system, Q. J. Roy. Meteor. Soc., 137, 553–597, 2011.

Eisen, O., Frezzotti, M., Genthon, C., Isaksson, E., Magand, O., van den Broeke, M. R., Dixon, D. A., Ekaykin, A., Holmlund, P., Kameda, T., Karlöf, L., Kaspari, S., Lipenkov, V. Y., Oerter, H., Takahashi, S., and Vaughan, D. G.: Ground-based measurements of spatial and temporal variability of snow accumulation in East Antarctica, Rev. Geophys., 46, RG2001, doi:10.1029/2006RG000218, 2008.

Favier, V., Agosta, C., Parouty, S., Durand, G., Delaygue, G., Gallée, H., Drouet, A.-S., Trouvilliez, A., and Krinner, G.: An updated and quality controlled surface mass balance dataset for Antarctica, The Cryosphere, 7, 583–597, doi:10.5194/tc-7-583-2013, 2013.

Frezzotti, M., Scarchilli, C., Becagli, S., Proposito, M., and Urbini, S.: A synthesis of the Antarctic surface mass balance during the last 800 yr, The Cryosphere, 7, 303–319, doi:10.5194/tc-7-303-2013, 2013.

Fujita, K. and Abe, O.: Stable isotopes in daily precipitation at Dome Fuji, East Antarctica, Geophys. Res. Lett., 33, L18503, doi:10.1029/2006GL026936, 2006.

Genthon, C. and Krinner, G.: Antarctic surface mass balance and systematic biases in general circulation models, J. Geophys. Res.-Atmos., 106, 20653–20664, 2001.

Genthon, C., Krinner, G., and Castebrunet, H.: Antarctic precipitation and climate change predictions: Horizontal resolution and margin vs plateau issues, Ann. Glaciol., 50, 55–60, 2009a.

Genthon, C., Magand, O., Krinner, G., and Fily, M.: Do climate models underestimate snow accumulation on the Antarctic plateau? A re-evaluation of/from in situ observations in East Wilkes and Victoria Lands, Ann. Glaciol., 50, 61–65, 2009b.

Gregory, J. and Huybrechts, P.: Ice-sheet contributions to future sea-level change, Philos T. R. Soc. A, 364, 1709–1732, 2006.

Haynes, J. M., L'Ecuyer, T. S., Stephens, G. L., Miller, S. D., Mitrescu, C., Wood, N. B., and Tanelli, S.: Rainfall retrieval over the ocean with spaceborne W-band radar, J. Geophys. Res.-Atmos., 114, D00A22, doi:10.1029/2008JD009973, 2009.

Hiley, M. J., Kulie, M. S., and Bennartz, R.: Uncertainty Analysis for CloudSat Snowfall Retrievals, J. Appl. Meteor. Climatol., 50, 399–418, 2010.

Kulie, M. S. and Bennartz, R.: Utilizing Spaceborne Radars to Retrieve Dry Snowfall, J. Appl. Meteor. Climatol., 48, 2564–2580, 2009.

Kumagai, H., Kuroiwa, H., Kobayashi, S., and Orikasa, T.: Cloud profiling radar for EarthCARE mission, Proc. SPIE, 4894, 118–125, 2003.

Lenaerts, J. T. M., van den Broeke, M. R., van de Berg, W. J., van Meijgaard, E., and Kuipers Munneke, P.: A new, high-resolution surface mass balance map of Antarctica (1979–2010) based on regional atmospheric climate modeling, Geophys. Res. Lett., 39, L04501, doi:10.1029/2011GL050713, 2012.

Liu, G.: Deriving snow cloud characteristics from CloudSat observations, J. Geophys. Res.-Atmos., 113, D00A09, doi:10.1029/2007JD009766, 2008.

Magand, O., Genthon, C., Fily, M., Krinner, G., Picard, G., Frezzotti, M., and Ekaykin, A. A.: An up-to-date quality-controlled surface mass balance data set for the 90–180° E Antarctica sector and 1950–2005 period, J. Geophys. Res.-Atmos., 112, D12106, doi:10.1029/2006JD007691, 2007.

Magand, O., Picard, G., Brucker, L., Fily, M., and Genthon, C.: Snow melting bias in microwave mapping of Antarctic snow accumulation, The Cryosphere, 2, 109–115, doi:10.5194/tc-2-109-2008, 2008.

Monaghan, A. J., Bromwich, D. H., Fogt, R. L., Wang, S.-H., Mayewski, P. A., Dixon, D. A., Ekaykin, A., Frezzotti, M., Goodwin, I., Isaksson, E., Kaspari, S. D., Morgan, V. I., Oerter, H., Van Ommen, T. D., Van der Veen, C. J., and Wen, J.: Insignificant Change in Antarctic Snowfall Since the International Geophysical Year, Science, 313, 827–831, 2006a.

Monaghan, A. J., Bromwich, D. H., and Wang, S.-H.: Recent trends in Antarctic snow accumulation from Polar MM5 simulations, Philos. T. R. Soc. A, 364, 1683–1708, doi:10.1098/rsta.2006.1795, 2006b.

Nakatsuka, H., Okada, K., Horie, H., Kimura, T., Iida, Y., Kojima, M., Sato, K., Ohno, Y., Takahashi, N., and Kumagai, H.: System Design of Cloud Profiling Radar for Earthcare, in: Geoscience and Remote Sensing Symposium, 2008, IGARSS 2008, IEEE International, Vol. 5, V-93–V-96, doi:10.1109/IGARSS.2008.4780035, 2008.

Rodgers, C.: Inverse methods for atmospheric sounding, vol. 2 of Series on Atmospheric, Oceanic and Planetary Physics, World Scientific, 2000.

Simmons, A., Uppala, S., Dee, D., and Kobayashi, S.: ERA-interim: new ECMWF re-analysis products from 1989 onwards, ECMWF Newslett, 110, 25–35, 2006.

Stephens, G. L., Vane, D. G., Tanelli, S., Im, E., Durden, S., Rokey, M., Reinke, D., Partain, P., Mace, G. G., Austin, R., L'Ecuyer, T., Haynes, J., Lebsock, M., Suzuki, K., Waliser, D., Wu, D., Kay, J., Gettelman, A., Wang, Z., and Marchand, R.: CloudSat mission: Performance and early science after the

first year of operation, J. Geophys. Res.-Atmos., 113, D00A18, doi:10.1029/2008JD009982, 2008.

Van de Berg, W., Van den Broeke, M., Reijmer, C., and Van Meijgaard, E.: Characteristics of the Antarctic surface mass balance, 1958–2002, using a regional atmospheric climate model, Ann. Glaciol., 41, 97–104, doi:10.3189/172756405781813302, 2005.

Wood, N. B.: Estimation of snow microphysical properties with application to millimeter-wavelength radar retrievals for snowfall rate., Ph.D. dissertation, Colorado State University, Fort Collins, Colorado, 231 pp., available at: http://hdl.handle.net/10217/48170, 2011.

Wood, N. B., L'Ecuyer, T., Vane, D. G., Stephens, G. L., and Partain, P.: Level 2C snow profile process description and interface control document, version 0, Tech. rep., http://www.cloudsat.cira.colostate.edu/ICD/2C-SNOW-PROFILE/2C-SNOW-PROFILE_PDICD_P_R04.pdf, 2013.